Antiproton-Proton Annihilation into Electron-Positron Pairs and Gamma-Ray Pairs*

D. L. HARTILL,† B. C. BARISH, D. G. FONG,‡ R. GOMEZ, J. PINE, AND A. V. TOLLESTRUP
California Institute of Technology, Pasadena, California 91109

AND

A. W. MASCHKE§
National Accelerator Laboratory, Batavia, Illinois 60510

AND

T. F. ZIPF§
Stanford Linear Accelerator Center, Stanford University, Stanford, California 94305

(Received 24 March 1969)

Experimental limits have been set on the cross sections for $\bar{p}+p \to e^+ + e^-$ for antiprotons with incident momenta of 1.47 and 2.40 GeV/c. These results imply upper limits on the magnitude of the proton form factors for timelike four-momentum transfer of 5.1 and 6.6 (GeV/c)^2. The reaction $\bar{p}+p \to \gamma+\gamma$ has been studied at the same incident momenta. This process has apparently been observed for incident antiproton momentum of 1.47 GeV/c, while an upper limit for the two-photon annihilation cross section is found at 2.40-GeV/c incident momentum.

I. INTRODUCTION

AN antiproton beam and counter spark chamber array have been used at the Brookhaven National Laboratory's alternating gradient synchrotron (AGS) to study the reactions

$$\bar{p}+p \to e^+ + e^-, \tag{1}$$

$$\bar{p}+p \to \gamma+\gamma \tag{2}$$

for incident antiproton momenta of 1.47 and 2.40 GeV/c.

The first reaction is related by crossing symmetry to

$$e^- + p \to e^- + p. \tag{3}$$

The pertinent lowest-order Feynman diagrams for reactions (1) and (3) are shown in Fig. 1. In the one-photon exchange approximation, if no structure is assumed for the $\gamma e^+ e^-$ vertex, the angular distribution of the electron in the annihilation reaction will directly yield the electric and magnetic form factors of the proton in the region of timelike four-momentum transfer squared q^2. These form factors are then functions of q^2 only in the one-photon approximation. The only previous experiment to determine the timelike form factors of the proton was carried out at the CERN Proton Synchrotron.[1] This experiment was done at $q^2=6.8$ (GeV/c)^2, and attempts were made to detect both electron pairs and muon pairs. No events were observed, and thus upper limits were set on the magnitudes of the form factors in the timelike region. The extensive electron-proton elastic scattering experiments[2] have given information on electric and magnetic form factors for spacelike momentum transfers.

In terms of the electric form factor $G_E(q^2)$ and the magnetic form factor $G_M(q^2)$ the differential cross section for the first reaction is given by[3]

$$\frac{d\sigma}{d\Omega}(\bar{p}p \to e^+e^-) = \frac{1}{16}\frac{\alpha^2}{E(E^2-M_p^2)^{1/2}} \times\left[|G_M(q^2)|^2(1+\cos^2\theta^*)+\left(\frac{M_p}{E}\right)^2 \times|G_E(q^2)|^2\sin^2\theta^*\right], \tag{4}$$

with

$\alpha = 1/137 =$ fine-structure constant,
$M_p =$ proton mass,
$q^2 = +2M_p(E+M_p)$,
$E =$ total energy of the $\bar{p}$ in the center-of-mass system,
$\theta^* =$ angle between $\bar{p}$ momentum vector and e^- momentum vector in the center-of-mass system,

and with

$$G_E(0)=1 \quad \text{and} \quad G_M(0)=1+\mu=2.79,$$

where $\mu =$ anomalous moment of the proton.

* Work supported in part by the U. S. Atomic Energy Commission. Prepared under Contract No. AT(11-1)-68 for San Francisco Operations Office, U. S. Atomic Energy Commission.

† Present address: Newman Laboratory of Nuclear Studies and Department of Physics, Cornell University, Ithaca, N. Y.

‡ Present address: Department of Physics, Brown University, Providence, R. I.

§ During the experiment, members of Accelerator Department, Brookhaven National Laboratory.

[1] M. Conversi, T. Massam, Th. Muller, and A. Zichichi, Nuovo Cimento **40A**, 690 (1965).

[2] T. Janssens, R. Hofstadter, E. B. Hughes, and M. R. Yearian, Phys. Rev. **142**, 922 (1966); E. B. Hughes, T. A. Griffy, M. R. Yearian, and R. Hofstadter, *ibid.* **139**, B458 (1965); M. Goitein, R. J. Budnitz, L. Carroll, J. Chen, J. R. Dunning, Jr., K. Hanson, D. Imrie, C. Mistretta, J. K. Walker, R. Wilson, G. F. Dell, M. Fortino, J. M. Patterson, and H. Winick, Phys. Rev. Letters **18**, 1016 (1967); W. Albrecht, H. J. Behrend, F. W. Brasse, W. Flauger, H. Hultschig, K. G. Steffen, *ibid.* **17**, 1192 (1966); D. H. Coward, H. DeStaebler, R. A. Early, J. Litt, A. Minten, L. W. Mo, W. K. H. Panofsky, R. E. Taylor, M. Breidenbach, J. I. Friedman, H. W. Kendall, P. N. Kirk, B. C. Barish, J. Mar, and J. Pine, *ibid.* **20**, 292 (1968).

[3] L. N. Hand, D. G. Miller, and R. Wilson, Rev. Mod. Phys. **35**, 335 (1963).

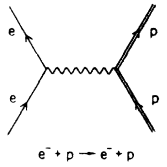

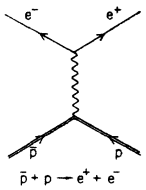

FIG. 1. Feynman diagrams for $e^-p \to e^-p$ and $\bar{p}p \to e^+e^-$ assuming one-photon exchange.

If the differential cross section has the dimensions cm²/sr, and if energies and masses are measured in GeV, the coefficient $\alpha^2/16$ becomes numerically equal to 1.33×10^{-33}. The cross section can also be written in terms of the Dirac and Pauli form factors F_1 and F_2, related to G_E and G_M by

$$G_E(q^2)=F_1(q^2)+(q^2/4M_p^2)\mu F_2(q^2), \quad (5)$$

$$G_M(q^2)=F_1(q^2)+\mu F_2(q^2). \quad (6)$$

They are mentioned here because if $F_2(q^2)$ is to remain finite at $q^2=4M_p^2$, the condition

$$G_E(4M_p^2)=G_M(4M_p^2) \quad (7)$$

must be satisfied. In addition, since the proton current operator is Hermitian, G_E and G_M must be real for spacelike momentum transfers; they can be complex, however, for timelike momentum transfers.

In the experiment to be described below, data were obtained for the electron-pair annihilation mode using antiprotons with momenta of 2.40 and 1.47 GeV/c. These momenta correspond to squared four-momentum transfers of 6.6 and 5.1 (GeV/c)², respectively.

Reaction (2) was studied not only for its own intrinsic interest, but also as a possible background to (1). No previous measurements of this reaction have been reported.

Basically, the hodoscopes and electronic circuitry for this experiment was designed to select out of all possible antiproton interactions only the following two-body reactions:

$$\bar{p}+p \to e^+ + e^-, \quad (8)$$

$$\bar{p}+p \to \pi^+ + \pi^-, \quad (9)$$

$$\bar{p}+p \to K^+ + K^-, \quad (10)$$

$$\bar{p}+p \to \bar{p}+p. \quad (11)$$

The results of measurements on reaction (11) have already been reported[4] and data from (9) and (10) will be published later. In the following paragraphs a general description of the apparatus will be given. Many of the characteristics of the apparatus which were pertinent for the present experiment were studied using reactions (9)–(11) because their comparatively high cross sections gave high counting rates.

Interactions (9)–(11) could be separately identified by accurately measuring the angles between the incoming beam and the outgoing particles. However, the angles for the $e^\pm$ state differ from those for the $\pi^\pm$ state by only a few tenths of a degree and, hence, reaction (8) was separated out by studying the electromagnetic interactions of the electrons in a combination of lead-plate spark chambers and lead Lucite Čerenkov counters.

A plan view and an end view of the apparatus are shown in Figs. 2 and 3. Two thin-plate spark chambers were placed symmetrically on the left and right sides of the target to record the paths of the final charged particles. Before spark-chamber pictures were taken, the directions of the final charged particles were determined roughly with six scintillation-counter hodoscopes. The channels in the outermost hodoscopes were horizontal and parallel to the target and provided a measurement of coplanarity. The other four hodoscopes had vertical channels and provided measurements of the angles between the final particles and the antiproton beam. The width of the channels in these hodoscopes was chosen so that they were able to distinguish between $\bar{p}$-p elastic events and e^+e^-, $\pi^+\pi^-$, K^+K^- annihilations. The spark chambers were triggered to record the tracks of charged particles only after (1) the hodoscopes determined roughly that the two charged particles in the final states were coplanar, that they were kinematically consistent with $e^\pm$ annihilations but not with $\bar{p}$-p elastic events, and (2) the Čerenkov counters indicated a large electromagnetic shower on both sides of the apparatus. Most of the unused solid angle was covered by veto counters.

II. EXPERIMENTAL APPARATUS

A. Antiproton Beam

The antiproton beam[5] used in this experiment was the long branch of a partially separated beam designed and built at Brookhaven National Laboratory's AGS.

The antiproton yield was

70 000/10^{12} protons in AGS at 2.40 GeV/c

and

30 000/10^{12} protons at 1.47 GeV/c.

At 2.40 GeV/c, the π^- and μ^- to $\bar{p}$ ratio was about 1.5 to 1, and the beam divergence was about $\pm0.6°$ at the hydrogen target. The momentum spread was about $\pm3.5\%$ of the mean beam momentum. The cross section of the beam at the target was oval-shaped, and

[4] B. Barish, D. Fong, R. Gomez, D. Hartill, J. Pine, A. V. Tollestrup, A. Maschke, and T. F. Zipf, Phys. Rev. Letters **17**, 720 (1966); **19**, 142(E) (1967).

[5] B. C. Barish and R. F. Kycia (to be published).

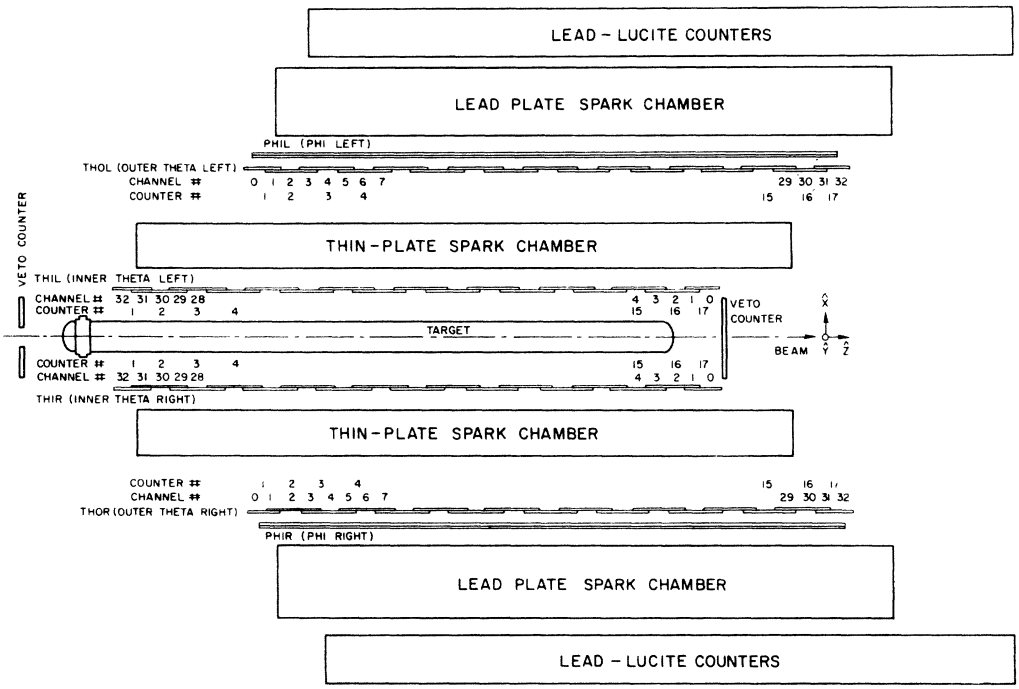

FIG. 2. Top view of the detection apparatus.

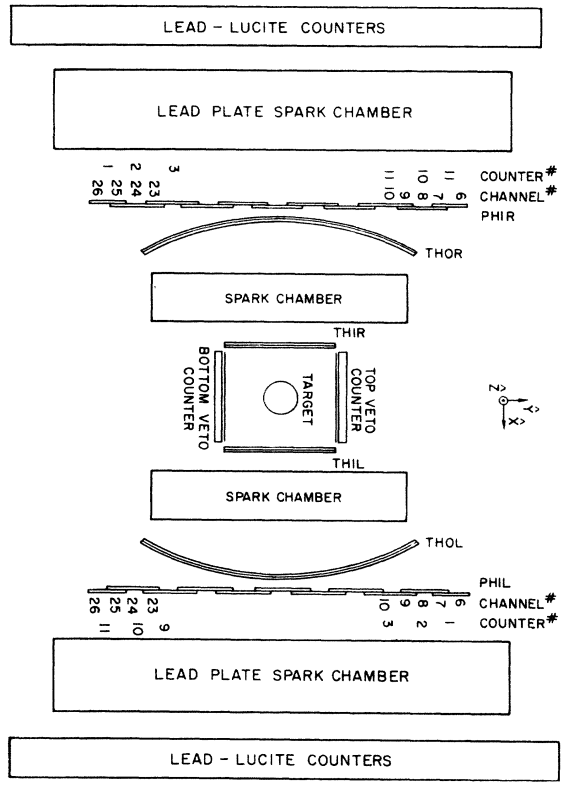

FIG. 3. End view of the detection apparatus.

was about 1 in.×2 in. depending somewhat on the beam momentum.

Antiprotons in the beam were identified by time of flight. The main contamination of π^-'s and μ^-'s was studied as follows at 2.40 GeV/c:

(a) When the electrostatic separators of the beam[5] were tuned to select π^- or μ^- mesons, it was found that the time-of-flight method to select anitprotons was able to discriminate against π^- or μ^- mesons with better than 99% efficiency.

(b) When the separators were tuned to select antiprotons, it was found that the antiproton to π^- or μ^--meson ratio at the target was about 1.5 to 1.

The conclusion was that, with the combined use of the separators and the time-of-flight method, the contamination of the antiproton count was less than 0.7%. At 1.40 GeV/c, it was expected to be even better because of the more effective time-of-flight selection.

After each antiproton was identified, a dead time of 4 μsec was imposed on the beam electronics. This was to prevent the spark chambers, which had a sensitive time of about 2.5 μsec, from recording simultaneously the final products of more than one $\bar{p}$-p interaction.

B. Target

Liquid hydrogen for the target was contained in a cylindrical Mylar flask of 4-in. diam and 82.5-in. length. The Mylar wall was 0.014 in. thick. The target was wrapped in 30 layers of superinsulation (crinkled 0.00025-in.-thick aluminized Mylar). It was suspended by thin stainless-steel wire hangers inside an evacuated

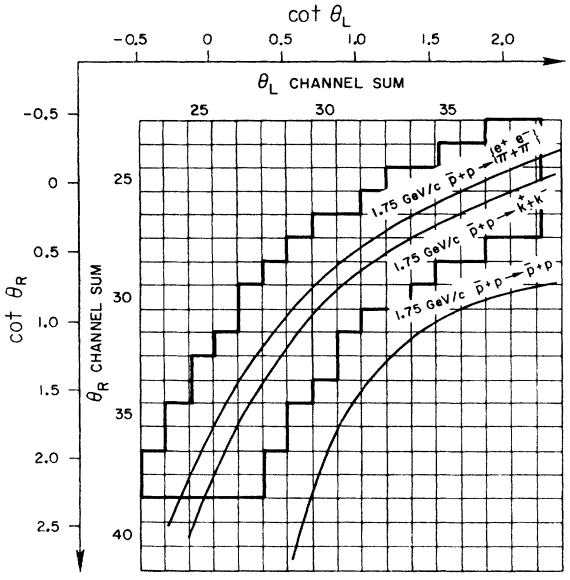

FIG. 4. θ_L-channel sum versus θ_R-channel sum matrix in $\cot\theta_L$ versus $\cot\theta_R$ space for $\phi=0$.

aluminum chamber with 0.014-in.-thick Mylar side walls. The liquid hydrogen was fed in and the gaseous hydrogen vented through a 2-in.-wide brass collar at the upstream end of the flask. The total usable length of the target was 80 in. The total material, besides the liquid hydrogen, through which a particle coming from the target had to pass to enter the detection hodoscopes was only 0.036 in. of Mylar. From the boiloff rate of the liquid hydrogen during the experiment, a calculation was made to set a limit on the correction to the liquid-hydrogen density due to gas bubbles. The hydrogen density in the target was found to be 0.069 g/cm^3.[6]

C. Hodoscope System

Six trays of scintillation counters were used in this experiment. Their positions relative to the hydrogen target are shown in Figs. 2 and 3. The setup was left-right symmetric. In order to minimize the required number of phototubes and to increase the efficiencies of the hodoscopes, the scintillators in each tray were overlapped as shown, and "channels" were defined by coincidence or anticoincidence between adjacent counters. All the scintillators in the hodoscopes were $\frac{1}{4}$ in. thick, and all the phototubes used were RCA 6655's.

The scintillators of the 11 counters in the outermost tray on each side were all 80 in. long. They were placed with their lengths parallel to the target and were 6.6 in. wide. They were overlapped to form 21 channels, each of 2.2-in. width, and each counter had a phototube on each end to increase the light collection efficiency. Five-bit binary numbers between 6 and 26 were generated electronically and corresponded to channels numbered as shown from top to bottom for both trays. These two hodoscopes, called the right and left ϕ trays, were placed equidistant (24 in.) from the axis of the target. They were used to impose a rough coplanarity condition on the particles coming from the target. A pair of tracks from the target axis, perfectly coplanar with the axis of the antiproton beam, would always strike the hodoscopes at two channels, whose sum was 32, independent of the inclination of the plane defined by these tracks. The sum of the two-channel binary numbers was generated by adding a six-bit adder. The output was decoded and the experiment triggered from sums of 31, 32, or 33, in order to include effects of channel width and beam size.

In each of the other hodoscopes, there were 17 counters, forming 33 channels of 2.5-in. width. The counters were placed vertically with their lengths perpendicular to the target, and each had one phototube at the bottom end. The scintillators of the innermost trays were straight, 13.5 in. tall and 6.5 in. from the axis of the target. They were called in inner-θ hodoscope trays. The middle trays, called the outer-θ trays, were curved, having a radius of curvature of 34 in. and were 22.2 in. from the axis of the target. They were 33.2 in. tall. The channels again electronically generated five-bit binary numbers between 0 and 32 from upstream to downstream for the outer-θ trays, and from downstream to upstream in the case of the inner-θ trays.

If a particle coming from the target passed through two θ trays, the sum of the channel numbers for the track was proportional to $\cot\theta$, where θ is the angle between the track and the direction of the incoming beam, and was independent of where the interaction took place along the target. This sum was made in six-bit binary adders in about 35 nsec. The purpose of having the outer θ counters curved was to eliminate the dependence of this sum on the azimuthal angle ϕ of the particle track. Thus, if the value of "channel sum" was made into a continuous rational number, this relationship could be expressed as

$$\text{channel sum} = 5.9\cot\theta + 25.3.$$

Figure 4 shows the θ-channel sum matrix in the $\cot\theta_{\text{right}}$-versus-$\cot\theta_{\text{left}}$ plane. For a definite antiproton beam momentum, the values of θ-left and θ-right for the process $\bar{p}+p \rightarrow$ (equal-mass pair) have a definite relationship. Thus, processes like (8)–(11) can be represented by single lines in the $\cot\theta_{\text{right}}$-versus-$\cot\theta_{\text{left}}$ plane, as shown in Fig. 4. The curves are for an incident antiproton momentum of 1.75 GeV/c.

In the CC1 (Caltech Computer 1), two five-bit binary encoders registered the values of the channel numbers for inner-θ and outer-θ hodoscopes on each side. These encoders were connected to the inputs of six-bit fast adders. The answers, corresponding to θ-channel sums 23–38, were used to drive each of the two sides of a 16×16 coincidence matrix corresponding

[6] D. L. Hartill, Ph.D. thesis, California Institute of Technology, 1967 (unpublished).

to a left-channel-sum–versus–right-channel-sum matrix. An output signal K (for "desired kinematics"), could be obtained from the CC1 if any one of a selected group of coincidence matrix elements was activated. For example, in Fig. 4, the squares inside the boundary marked by the heavy line represent the coincidence matrix elements (K matrix) for selecting $e^{\pm}$, $\pi^{\pm}$-pair, and $K^{\pm}$-pair events at an antiproton momentum of 1.75 GeV/c. With this K matrix, the $\bar{p}$-p elastic scattering events could thus be completely eliminated, while high efficiency was maintained for the desired events.

D. Shower Counters

Lead-Lucite Čerenkov counters of the type described by Heusch and Prescott[7] were placed behind the outer lead-plate spark chambers. These chambers provided approximately four radiation lengths of lead in which a shower could develop before entering the shower counters. The response of the lead-Lucite Čerenkov counters to electrons was determined by using electrons selected from the antiproton beam by means of a gas-filled Čerenkov counter. For this calibration procedure the counters were placed in the beam, and energies and angles of incidence of the electrons on the counter array were matched with the electron kinematics in the annihilation process. A pulse-height criterion was chosen for these counters such that pion pairs and many other types of events were effectively rejected. The electron-detection efficiency of the entire array of Čerenkov counters was $\geq 92\%$. The gains of each of the 40 5-in. photomultiplier tubes attached to these counters were checked weekly by means of Sr^{90} sources irradiating a $\frac{1}{16}$-in. scintillator glued to the light pipes of each of the Čerenkov counters. The pulse-height spectrum from a given tube was compared with a standard spectrum from the tube. The maximum observed variation in gain was less than 4% during the course of the experiment.

E. Spark Chambers and Camera System

Two thin-plate spark chambers were used for observing the paths of the charged particles in the final states. They were placed symmetrically, one on each side of the target, as shown in Figs. 2 and 3.

In each chamber, there were nine plates, each consisting of 0.001-in.-thick tempered aluminum foil, stretched and bonded over a 3-in.-wide aluminum frame with dimensions $\frac{3}{8}$ in.$\times$38 in.$\times$96 in. The plates were separated by 0.340-in.-thick Lucite spacers, forming eight gaps. The side walls of the chambers were of 0.014-in.-thick Mylar sheets. These chambers were viewed by three cameras, one 16 ft above each chamber, and one 32 ft away downstream, viewing both chambers. On the end of each chamber was a field lens consisting of a section of a spherical lens of focal length 32 ft. Lucite prisms were placed over each gap in the top view to bend the light into the camera.

The outer-shower chambers consisted of 0.11-radiation-length lead plates arranged at 50° to the beam direction in a herringbone pattern, so that particles from the target traversed the plates as close to their normal as possible. A shower could thus be seen in about 30 gaps before leaving the chambers.

A plastic field lens filled with mineral oil[8] was located on top of each chamber, and a mirror system combined the right and left chamber into one view for the camera. Lights recorded which hodoscope counters were triggered by the event, to make it easy to identify the shower with the proper particle. Only the vertical view of these chambers was photographed.

F. Triggering Requirements

The fast electronics described above had an over-all delay of about 150 nsec and were used to fire the spark chambers provided that (1) none of the veto counters were hit, (2) only one particle passed through each of the θ and ϕ hodoscope trays of counters, (3) the ϕ hodoscope coplanarity requirement was satisfied, (4) the θ hodoscopes gave an event in the acceptable region of the kinematics (K) matrix, and (5) there was a larger pulse in each of the shower counters. When the chambers were fired, the serial number of the event, the pulse height of the two shower counters, and those counters in the hodoscope which were triggered were recorded for future analysis.

In the electron-positron measurement, the spark-chamber trigger rate was about one per 4×10^5 antiprotons traversing the target (of which more than 10^5 interacted) at an antiproton momentum of 2.40 GeV/c. At 1.47 GeV/c, the trigger rate was about three times higher, mainly because of the large number of pion pairs.

The elements of the fast electronics were monitored continuously by a PDP-5 digital computer. When the fast electronics accepted an event, this device stored the relevant addresses of the scintillation counters in the hodoscopes and the coincidence channels. The computer was programmed to present, in matrix format and both in printed form and as oscilloscope display, the distributions of counts in the various addresses. For example, it could present the θ hodoscope data (there were 16 legal inner- and outer-θ counter channels on each side of the target) as a 16$\times$16 matrix. An element of this matrix represented the number of events in which the particle on the right of the target formed an angle with the incident-beam direction of θ_R and that on the left formed the angle θ_L. In addition to the data from the scintillation counters, the computer stored, according to the number of the counter, the pulse heights of the lead-Lucite Čerenkov counters. At frequent and periodic intervals during the course of the data-taking runs, the data in the computer were

[7] C. A. Heusch and C. Y. Prescott, Nucl. Instr. Meth. 29, 125 (1964).

[8] J. Pine, California Institute of Technology Internal Report No. 14, 1965 (unpublished).

TABLE I. Summary of Monte Carlo calculations of the solid-angle acceptance of the detection apparatus for electron-positron pairs and γ pairs. The last three rows are calculated using the Rosenbluth formula[6] and apply only to electron-positron annihilations. The units are steradian meters (i.e., target-length $\times$ fractional solid angle).

Form of angular distribution	Beam momentum 1.47 GeV/c	2.40 GeV/c
Isotropic	$(0.772\pm0.030)\pi$	$(0.957\pm0.034)\pi$
$G_E=G_M/(1+M)=G_M/2.79$	$(0.640\pm0.026)\pi$	$(0.765\pm0.030)\pi$
$G_E=G_M$	$(0.664\pm0.030)\pi$	$(0.794\pm0.030)\pi$
$G_E=0$	$(0.616\pm0.025)\pi$	$(0.736\pm0.030)\pi$

printed and compared with those from previous runs. Standard runs on $\bar{p}$-p elastic scattering were used. As a result of this procedure, failures in the rather large and complex electronics system could be located and corrected relatively soon after they occurred.

The data from the counter system and the spark-chamber photographs were correlated by a data-display system which was run in parallel with the PDP-5. This system drove an IBM model 526 card punch and a system of lights which were photographed with the spark chambers. All counter and coincidence-channel data pertinent to the event were punched on the IBM card associated with that event. The system of lights consisted of illuminated numbers placed adjacent to each of the elements of the θ and ϕ hodoscopes. The appropriate lights were activated when the spark chambers were fired. Then lights were used later, as an aid in scanning the film.

The angular resolution achieved with the thin-plate spark chambers for single tracks was better than ±1 degree. In the electron-positron annihilation experiment, this was sufficient to distinguish electron-pair events from K-pair events, but not from pion-pair events. For the latter, an angular accuracy of ~0.1 degree would have been required.

The response of the outer lead-plate chambers to electrons was determined by using electrons selected from the beam by the gas Čerenkov counter. The method used here was similar to that used to calibrate the lead-Lucite counters. In particular, measurements were made with the chambers oriented such that the angle of incidence of the electron and its momentum corresponded to that of an electron originating in the annihilation process. At these angles the spark chambers were typically four radiation-lengths thick. From these measurements, scanning criteria were devised such that each chamber provided better than 1000:1 rejection for pions. At the same time, an electron-detection efficiency of $91\pm3\%$ was retained. Thus, the requirement that each particle simulate an electron gave a probability of less than 10^{-6} that a pion pair could be confused with an electron pair. After the electron-pair and γ-pair data had been taken, the lead-Lucite Čerenkov counter requirement on the spark-chamber trigger was removed, and the apparatus used to take data for a measurement of the two-pion annihilation cross section. The results of this measurement have been published elsewhere,[9] and they indicate that the background from a pion pair masquerading as an electron pair is negligible. As a further check on the pion-rejection ratio in the lead spark chambers, 1900 known pion-pair annihilations were scanned using the electron criteria. Only one pion "shower" in this sample of 3800 pion tracks effectively simulated an electron.

The modification of the above system to measure the two-photon annihilation cross section was accomplished by placing a $\frac{1}{4}$-in. lead sheet, supported by $\frac{1}{8}$-in. aluminum, between the inner elements of the θ hodoscope and the thin-plate spark chambers. The electronic logic for event selection was modified such that the inner elements of each θ hodoscope were run in the veto mode. Appropriate pulses were then required from the counters in the outer elements of the θ hodoscopes, the ϕ hodoscopes, and the Čerenkov counters. Only events with both γ rays converting in the lead sheets to give narrow-angle e^+e^- pairs were analyzed. For this portion of the experiment, the lead-sheet spark-chamber array was calibrated by placing it in a tagged-photon beam obtained from the California Institute of Technology Electron Synchrotron. Measurements were made on photographs of showers originating from photons, with energies ranging 50 MeV–1.2 GeV. The over-all detection efficiency for the reaction $\bar{p}+p\rightarrow\gamma+\gamma$ was determined to be $(6.5\pm2.0)\times10^{-3}$.

The detection apparatus was sensitive to annihilations from 60° to 120° in the center-of-mass system. The solid-angle acceptance of the system was calculated for the e^++e^- final state using the California Institute of Technology IBM model 7094 computer. A Monte Carlo type of statistical method was used. To check the validity of this calculation, the solid angle for a flat center-of-mass angular distribution was calculated, using scale drawings of the apparatus, by measuring the actual target length from which the final state could be detected. The graphical results and the results from the computer program agreed to within 5%.

The solid-angle calculations included the beam attenuation in the target, the expected center of angular distribution, and the Čerenkov-counter detection efficiency. Additional effects, such as the spreading of the electron showers and the uncertainty of the correct sensitive area of the Čerenkov counters, led to systematic uncertainties of the order of 10%. The results of the solid-angle calculations are given in Table I.

III. DATA ANALYSIS

The scanning of the film from the electron-positron annihilation part of the experiment was carried out in four steps. In each succeeding step more stringent requirements were placed on the events. These steps were as follows:

[9] D. G. Fong, Ph.D. thesis, California Institute of Technology, 1968 (unpublished).

TABLE II. Summary of scanning and measuring of film for electron-positron and $\gamma\gamma$ final states.

Reaction	Beam momentum (GeV/c)	Total pictures	(Step 1) Showerlike events	(Step 2) Rough shower	(Step 3) Kinematics	(Step 4) Final analysis of showers
$\bar{p}+p \rightarrow e^+e^-$	1.47	58 000	1600	144	26	2
	2.40	26 000	500	49	7	0
$\bar{p}+p \rightarrow \gamma+\gamma$	1.47	1 990	85	...	2	2
	2.40	932	30	...	0	0

Step 1. Both lead chambers have "showerlike" tracks, starting within three gaps of the front of the chambers, which had spark counts greater than the mean number of sparks for a straight track plus ten sparks.

Step 2. Those events surviving step 1 were further required to have in the lead chambers (a) no additional straight tracks or tracks with a single scatter coming from the same vertex in the target as the "shower"; (b) at most, one converting γ ray in addition to the "shower" in each chamber to allow for γ rays arising from secondary radiation processes; (c) no single vertices in the "shower." From the calibration runs, pion interactions gave rise to single vertices, while electron showers did not; (d) "showers" which were continuous; i.e., they could not have breaks with no sparks for four or more consecutive gaps. Such a break could arise from a pion charge-exchange interaction in one of the plates.

Step 3. The tracks of events surviving step 2 were spatially reconstructed using the photographs of the thin-foil chambers. The allowable limits of deviation of the measured kinematical results from the calculated ones were very accurately determined from the analysis of 40 000 photographs taken when the apparatus was used to measure the annihilation of antiprotons into pion and kaon pairs. These limits were that the event be coplanar to $\pm 1.6°$, that the distance of closest approach of the reconstructed tracks inside the hydrogen target be less than 1 in., and that the computed (mass)^2 of the final particle be between -0.10 (GeV/c)^2 and $+0.10$ (GeV/c)^2. These limits correspond to a 95% efficiency cut. The energy loss of the antiproton in the liquid hydrogen up to the point of interaction was included in these calculations.

The information from the spatial reconstruction of the events was also used to predict which counters in the hodoscopes should have been traversed. If this prediction did not agree with the punched card for that event, the event was remeasured.

Step 4. The showers of the relatively small number of events surviving Step 3 were then analyzed in detail. In addition to the rough requirements in step 2, the showers were required (a) to be symmetric, within statistics, about the incident-particle direction, (b) to have no straight-track core which would be characteristic of a converted γ ray superimposed on a straight track; (c) to have no track or tracks at an angle greater than 45° to the shower direction, (d) to have single sparks in the first or second gap of the lead-plate chambers, in order to eliminate narrow-angle pairs which appeared as single tracks in the thin-foil chambers and γ rays which converted early in the lead chambers, and (e) to have projected polar angles ($\phi=0$ plane) of the mean direction of both showers, with $\pm 4°$ of the angle determined from the spatial reconstruction.

At 2.40 GeV/c, no events were found which satisfied all of the above criteria; however, the 1.47-GeV/c data yielded two acceptable candidates. Table II summarizes the number of events remaining after each step of the scanning for both the electron-positron final state and the $\gamma\gamma$ final state.

The film for the $\gamma\gamma$ final state was scanned first by looking for events with either one or two showers in both lead-plate chambers. The tracks in the thin-foil chambers from which the showers originated were then measured and the events reconstructed in space. Only events with pairs coming from the lead converter having less than a 10° opening angle were measured. In the single-track case, the direction of the γ ray was assumed to be the direction of the track, and in the two-track case it was assumed to be the bisector of the two tracks. The measured events were then analyzed with the same method that was used for the e^+e^- final state. At 2.40 GeV/c, no events were found, and at 1.47 GeV/c, two candidates satisfied all the event criteria.

The scanning and measuring was carried out twice on all of the film and three times on half of the film. From these rescans, the total scanning efficiency for both portions of the experiment was determined to be greater than 98%.

IV. BACKGROUNDS

In addition to the possible background from charged-pion pairs mentioned above, annihilations of antiprotons which produce γ rays can simulate e^+e^- events. These γ rays can come either directly from the annihilation or from the decay of π^0's produced in the annihilation. If two charged pions are produced in an annihilation such that they have the kinematics of an e^+e^- event, and two γ rays from the annihilation convert in the lead-plate chambers so that their showers overlap the charged-pion tracks, then it could simulate an e^+e^- event. In annihilations that produce only π^0's and γ rays, it is possible for two of these γ rays to convert

TABLE III. Summary of the background analysis for the data taken using 1.47-GeV/c incident antiprotons.

Annihilation mode	Cross section $\left[\left.\frac{d\sigma}{d\Omega}\right\|_{90°}$ (cm²/sr)$\right]$	Background $\left[\left.\frac{d\sigma}{d\Omega}\right\|_{90°}$(cm²/sr), 90% confidence level$\right]$
$\bar{p}+p \rightarrow \gamma+\gamma$	$(1.6_{-0.8}^{+1.9})\times10^{-31}$	$\pi^0+\pi^0 \leq 0.1\times10^{-31}$
		$\pi^0+\gamma \leq 0.3\times10^{-31}$
		total $\leq 0.4\times10^{-31}$
$\bar{p}+p \rightarrow e^+e^-$	$(1.2_{-0.6}^{+1.1})\times10^{-34}$	$\pi^+\pi^- \leq 1.5\times10^{-35}$
		$\pi^+\pi^-+n\pi^0 \leq 1.4\times10^{-35}$
		$\pi^0+\pi^0 \leq 3.1\times10^{-35}$
		$\pi^0+\pi^0 \leq 3.1\times10^{-34}$
		$\pi^0+\gamma \leq 0.8\times10^{-35}$
		$\gamma+\gamma = (1.3_{-0.65}^{+1.5})\times10^{-34}$
		total $= (1.6_{-0.7}^{+1.8})\times10^{-34}$

into a very narrow-angle e^+e^- pair in the material of the liquid-hydrogen target (=0.037 radiation lengths). These pairs would then appear as single tracks in the kinematics chambers and produce bona fide showers in the lead-plate chambers. The most serious background process of this type would be the $\gamma\gamma$ process, since the γ rays already have the correct kinematics.

Since only the top view of the lead-plate chambers was available, the γ-ray and charged-pion track only had to overlap in this view. Electron showers characteristically do not have a straight track as core of the shower, so final candidates with showers containing a straight track core were rejected. However, detailed questions of track efficiency may affect the reliability of this procedure. To check this, the spatial distribution of events in the data, in which a single track and a shower appeared in the same lead-plate chamber, was determined as a function of the separation between the track and the shower. This distribution was then extrapolated to zero separation. Since the minimum observable horizontal separation was 0.1 in., the probability that an annihilation of the type $\bar{p}+p \rightarrow \pi^+\pi^-+n\pi^0$ could simulate an e^+e^- event was directly determined from this distribution to be less than 5×10^{-6}.

Annihilations which produce only π^0's and γ rays also are a background for the $\gamma\gamma$ experiment. If two of the γ rays materialize in the lead converter, have the proper kinematics for the $\gamma\gamma$ final state, and the remaining γ ray(s) escape(s) detection, then this annihilation would simulate a $\gamma\gamma$ event.

Prior to this experiment, no data on neutral annihilations of antiprotons in the several-GeV/c momentum range were available. Therefore, at the end of the data-taking runs, the apparatus was triggered on events in which there were no charged particles passing through the scintillation counters but with pulse heights comparable to those for electron showers appearing in the Čerenkov counters. In events of high photon multiplicity, the efficiency for detecting all of the photons was quite low. Thus, the measurement of these types of events is such that the events with the greater number of γ rays form backgrounds for the events with fewer γ rays. Although the nature of the apparatus was such that this attempt to measure these cross sections was crude, it was possible to obtain upper limits on the differential cross section at 90° in the center-of-mass system for those reactions which represented the more serious backgrounds. These cross sections were then used in a Monte Carlo type of analysis to predict the background for the experiment. The computer program which was employed included the spatial distribution of the antiproton beam and the detection efficiency of the veto counters for γ rays, and required that the γ rays which struck the Čerenkov counters have an energy greater than 20 MeV.

The only final candidates for either of the reactions under study occurred at 1.47 GeV/c. For this reason a detailed study of the background was carried out only for events arising from antiprotons of this momentum. The result of this analysis indicated that the more serious background reactions for the $\gamma\gamma$ measurement were the annihilation into $2\pi^0$ and $\pi^0\gamma$ final states. For the $\gamma\gamma$ final state, the over-all background cross section due to the $2\pi^0$ and π^0 final states was determined to be

$$\frac{d\sigma}{d\Omega_{90°}}(\bar{p}p \rightarrow 2\gamma)_{\text{fake}} = (2.7\pm0.6)\times10^{-32}\ \text{cm}^2/\text{sr}. \quad (12)$$

In the e^+e^- case, the more serious backgrounds arise from the annihilation into $2\pi^0$, $n^0\gamma$, and 2γ. The most serious of these is the $\gamma\gamma$ reaction, for which two candidates remained after the final scan of the data. If these events are real, then the expected background cross section from this reaction at 1.47 GeV/c antiproton momentum would be

$$\frac{d\sigma}{d\Omega_{90°}}(\bar{p}p \rightarrow e^+e^-)_{\text{fake}} = (1.3_{-0.65}^{+1.5})\times10^{-34}\ \text{cm}^2/\text{sr}. \quad (13)$$

The total estimated background, including the $2\pi^0$ and $\pi^0\gamma$ annihilations, is estimated as

$$\frac{d\sigma}{d\Omega_{90°}}(\bar{p}p \rightarrow e^+e^-)_{\text{fake}} = (1.6_{-0.7}^{+1.5})\times10^{-34}\ \text{cm}^2/\text{sr}. \quad (14)$$

In Table III, the background cross-section estimates for these measurements are given for the runs at 1.47-GeV/c antiproton momentum.

The cross sections for the $2\pi^0$ and $\pi^+\pi^-$ fall by about an order of magnitude as the incident antiproton momentum is increased from 1.47 to 2.40 GeV/c. If this cross-section dependence upon momentum is used as a scaling factor, then the background cross-section estimates for the 2.40-GeV/c runs are

$$\frac{d\sigma}{d\Omega_{90°}}(\bar{p}p \rightarrow 2\gamma)_{\text{fake}} \cong 3\times10^{-33}\ \text{cm}^2/\text{sr} \quad (15)$$

TABLE IV. Differential cross sections (cm²/sr) at 90° in the center-of-mass system.

$\bar{p}$ momentum (GeV/c)	Four-momentum transfer [(GeV/c)²]	$p+p\to e^+e^-$	$p+p\to\gamma+\gamma$
1.47	5.1	$<1.8\times10^{-34}$	$(1.6_{-0.8}{}^{+1.9})\times10^{-31}$
2.40	6.8	$<4.2\times10^{-35}$	$<0.8\times10^{-31}$

and

$$\frac{d\sigma}{d\Omega_{90°}}(\bar{p}p\to e^+e^-)_{\text{fake}}\cong 1.3\times10^{-35}\ \text{cm}^2/\text{sr}. \quad (16)$$

V. DISCUSSION

The results of this experiment can be used to set limits on G_M, assuming values for G_E/G_M. For annihilation at rest, it is necessary that $G_E/G_M=1$ if the Pauli form factor F_2 remains finite. Assuming this value for the ratio of G_E to G_M, this experiment establishes the following 90% confidence upper limits:

$$\begin{aligned} &G_M<0.16 \quad \text{at} \quad q^2=6.6\ (\text{GeV}/c)^2,\\ &G_M<0.20 \quad \text{at} \quad q^2=5.1\ (\text{GeV}/c)^2. \end{aligned} \quad (17)$$

For spacelike four-momentum transfers, there is no evidence against $G_E/G_M=1/\mu_p=1/2.79$, the "scaling law." With this ratio we obtain the following 90% confidence upper limits:

$$\begin{aligned} &G_M<0.18 \quad \text{at} \quad q^2=6.6\ (\text{GeV}/c)^2,\\ &G_M<0.24 \quad \text{at} \quad q^2=5.1\ (\text{GeV}/c)^2. \end{aligned} \quad (18)$$

These results are consistent with the results at $q^2=6.8$ (GeV/c)² obtained from the CERN experiment. The limit established in the experiment described in this paper is essentially the same as the combined limit from the muon and electron data of Conversi *et al.*,[1] and about a factor of 2.5 lower than their limit based on electron data alone.

Various models have been proposed to fit the abundant electron scattering data which have been used to determine the spacelike form factors, and the data presented here can limit the choice of models to those with acceptable timelike behavior. For example, the well-known "dipole" fit

$$\frac{G_M}{\mu}=\left(\frac{1}{1-q^2/0.71}\right)^2 \quad (19)$$

is consistent with the limits established by this experiment.

The measured cross section for γ-pair annihilation is about 30 times larger than would be predicted for annihilation of "Dirac protons," with no structure and no anomalous moment. An estimate for the cross section for the γ-pair annihilation mode might be derived by considering that it proceeds via virtual ρ and ω pairs,

$$p+p\to\begin{bmatrix}\rho^0+\rho^0\\ \rho^0+\omega^0\\ \omega^0+\omega^0\end{bmatrix}\to\gamma+\gamma. \quad (20)$$

Very crudely, the γ-pair cross section might be down by a factor $(\alpha)^2$ from the sum of these boson-pair cross sections. While these have not been measured in flight, at rest they are known to constitute about 1% of the total annihilations.[10] If, at 1.47 GeV/c, they still constitute about 1% of the annihilations, they then account for a cross section of about 0.5 mb. Reducing this by a factor $(\alpha)^2$, and assuming an isotropic angular distribution, gives a cross section of 2×10^{-32} cm²/sr. This number is low by nearly an order of magnitude. A more careful calculation, assuming the vector-dominance model, has been done by Zweig.[11] According to this calculation, the predicted γ-pair yield is even smaller, equal to about 20% of α^2 times the boson-pair cross section.

The γ-pair cross section was, as discussed above, subject to sizable backgrounds. It is possible, though it appears unlikely, that the γ-pair cross section has been overestimated and that one or both of the electron pairs observed at 1.47 GeV/c is a bona fide event.

ACKNOWLEDGMENTS

We wish to thank John Madey, John Gallivan, Peter Mazur, Jerome Mar, Ken Young, and Edward Olsen, all of the California Institute of Technology, for their help with the experiment. We are grateful to many people at Brookhaven National Laboratory for their help and hospitality. Particularly, we would like to thank T. Blair, R. Gibbs, A. P. Schlafke, J. Hennesy, J. Lepicki, Dr. J. R. Sanford, and the members of the AGS crew. Two of us (A.W.M. and T.F.Z.) wish to thank Dr. Lyle Smith for the generous assistance which he provided during the early stages of the experiment.

[10] C. Baltay, N. Barash, P. Franzini, N. Gelfand, L. Kirsch, G. Lütjens, D. Miller, J. C. Severiens, J. Steinberger, T. H. Tan, D. Tycko, D. Zanello, R. Goldberg, and R. J. Plano, Phys. Rev. Letters **15**, 532 (1965).

[11] G. Zweig (private communication).